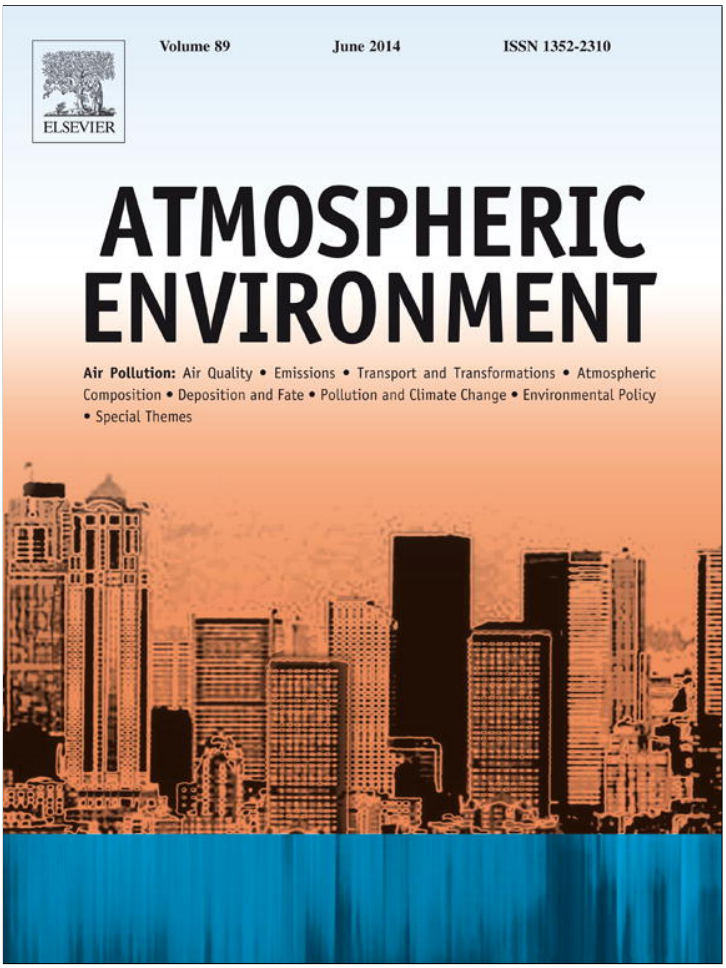

Atmospheric Environment 89 (2014) 298–308

Contents lists available at ScienceDirect

Atmospheric Environment

journal homepage: www.elsevier.com/locate/atmosenv

An unconventional adaptation of a classical Gaussian plume dispersion scheme for the fast assessment of external irradiation from a radioactive cloud

Petr Pecha [a,*], Emilie Pechova [b]

[a] Institute of Information Theory and Automation of the Czech Academy of Sciences, v.v.i., Pod Vodarenskou vezi 4, 182 08 Prague 8, Czech Republic
[b] Institute of Nuclear Research, Div. EGP, 250 68 Rez near Prague, Czech Republic

HIGHLIGHTS

- A new effective procedure for finite cloud dose estimation at near distances.
- Capability of real-time simulation of responses at a large sensor networks.
- Substitution of multi-nuclide scheme to effective photon multi-group design.
- Incorporation into environmental model HARP and comparison benchmarks.
- Supports assimilation of model predictions with observations from terrain.

ARTICLE INFO

Article history:
Received 9 July 2013
Received in revised form
20 December 2013
Accepted 3 January 2014
Available online 23 January 2014

Keywords:
Photon fluence
Atmospheric dispersion
Cloudshine dose

ABSTRACT

This article focuses on derivation of an effective algorithm for the fast estimation of cloudshine doses/dose rates induced by a large mixture of radionuclides discharged into the atmosphere. A certain special modification of the classical Gaussian plume approach is proposed for approximation of the near-field dispersion problem. Specifically, the accidental radioactivity release is subdivided into consecutive one-hour Gaussian segments, each driven by a short-term meteorological forecast for the respective hours. Determination of the physical quantity of photon fluence rate from an ambient cloud irradiation is coupled to a special decomposition of the Gaussian plume shape into the equivalent virtual elliptic disks. It facilitates solution of the formerly used time-consuming 3-D integration and provides advantages with regard to acceleration of the computational process on a local scale. An optimal choice of integration limit is adopted on the basis of the mean free path of γ-photons in the air. An efficient approach is introduced for treatment of a wide range of energetic spectrum of the emitted photons when the usual multi-nuclide approach is replaced by a new multi-group scheme. The algorithm is capable of generating the radiological responses in a large net of spatial nodes. It predetermines the proposed procedure such as a proper tool for online data assimilation analysis in the near-field areas. A specific technique for numerical integration is verified on the basis of comparison with a partial analytical solution. Convergence of the finite cloud approximation to the tabulated semi-infinite cloud values for dose conversion factors was validated.

1. Introduction

The main goal of this article is to formulate a fast and sufficiently accurate approach for estimation of the cloudshine irradiation doses which replaces the former rough estimations. The shape of a radioactive plume in the atmosphere near the source of pollution is narrow (especially for a stable atmospheric stratification like category *F*) and does not noticeably diffuse to the surface until it has travelled a distance of several kilometres from the point of discharge (even more than 10 km for a buoyant plume). Due to the buoyant and vertical momentum plume rise the effective height can markedly increase. The vertical concentration profile is gradually getting homogenous only from greater distances. Common practice introduces the calculation of the ground-level cloudshine dose rates at larger distances as a product of this homogenised near-ground activity concentration and the tabulated conversion

* Corresponding author.
E-mail address: pecha@utia.cas.cz (P. Pecha).

1352-2310/$ – see front matter © 2014 Elsevier Ltd. All rights reserved.
http://dx.doi.org/10.1016/j.atmosenv.2014.01.007

coefficient R_{cloud} (Sv m^3 Bq^{-1} s^{-1}) defined in (ICRP 74, 1996). The technique of the irradiation calculations is designated as a semi-infinite cloud approach. Its application at near distances can, however, cause huge errors and the real finite plume shape should be respected. Further development led to the time-consuming calculations based on a three-dimensional integration over the finite cloud volume (e.g. ADMS4, 2009; Overcamp, 2007) or on a specially partitioned integration space (Wang et al., 2004; Raza et al., 2001). The 3-D integration of the Gaussian plume is fairly complex and computationally expensive, and in many cases sufficiently accurate approximations could be constructed. The volume integral for gamma doses was formerly approximated by using the semi-infinite cloud model combined with correction factors. The first attempt to solve the problem was the former approach based on introduction of a certain tabulated finite cloud correction factors F^{cor} (Slade, 1968). The similar approach based on a pre-calculated matrix of the cloud gamma correction factors was used in (Päsler-Sauer, 2000) – parameterisation in the photon energy, horizontal dispersion coefficient, roughness length, plume height, and stability class. An analogical procedure is used in (Thykier-Nielsen et al., 1995) in the Lagrangian puff model RIMPUFF for the calculation of gamma doses from asymmetrical puffs. The multi-parameter gamma dose values are pre-calculated as a function of the photon energy, horizontal dispersion and asymmetry factor, height of puff centre and the distance from the puff base point. We have two main objections to the pre-calculated procedures. Firstly, due to the steep gradients of activity concentration a suitable interpolation on the fixed spatial grid could be problematic. Secondly, we have to include possible elevated locations of the receptors (e.g. real orography of the terrain, monitoring towers). Our proposed method inherently solves the 3-D configuration of the receptors, which can be crucial for the determination of a dangerous flight levels for an aircrew during the aerial monitoring.

An ultimate aim of our research is improvement of the model predictions of this radiological situation based on assimilation with real observations incoming from the terrain. The assimilation procedures perform statistical merging of the model predictions and the measured values in the observation space. Its dimension equals the number of monitoring sensors on the terrain and, therefore, a parallel simulation of the dose rate responses on a large net of receptors in the terrain from a wide group of leaking radionuclides is essential. At the same time some special online examinations like predicting the time to the first alarm or investigating the weakest plume detectability can be accomplished. From a general point of view the fast and effective method for estimation of the finite cloud problem at near distances facilitates the realisation of the assimilation techniques. Advanced assimilation techniques coming from sequential Monte-Carlo methods are computationally expensive (e.g. Doucet et al., 2001) and an effective procedure for fast simulation of external irradiation has a crucial significance (ASIM, 2012). Our first attempts at Bayesian tracking began in (Pecha et al., 2009). The recent application of inverse modelling techniques for extracting of the model parameter information from the incoming terrain observations is described in (Šmídl et al., 2013).

2. Predictions of harmful admixture propagation nearby a source

This article deals with adaptation of the classical solution of a diffusion equation in the initial phase of radioactive plume drifting. The analysis should satisfactorily cover the area of a teledosimetric ring of sensors (TDS) located within a few hundred metres around a source. The 3-D distribution of the specific radioactivity concentration C^n of nuclide n in the air (Bq m^{-3}) is expressed by the straight-line Gaussian solution. This near-field model has a long tradition of use for dispersion predictions. Even though it is simple, the Gaussian model is consistent with the random nature of turbulence (Hanna et al., 1982). It is a solution of the Fickian diffusion equation for constant diffusivity coefficient K and average plume velocity $\bar{u}$. The model is tuned to experimental data and offers quicker estimation with a reasonable computational effort. Proved semi-empirical formulae are available for approximation of important effects such as interaction of the plume with *near-standing buildings* or momentum and buoyant *plume rise* during release. Semi-empirical formulae are introduced for estimation of the wind speed *changes with height* and for *depletion* of the plume radioactivity due to the *removal processes* of dry and wet deposition and radioactive decay. Separate transport mechanisms of radioactivity according to the *physical–chemical forms* of admixtures and *landuse characteristics* are considered. The effects of small changes of *surface elevation* and *terrain roughness* on atmospheric dispersion can be approximately included.

Let assume the continuous radioactivity release to be decomposed into consecutive time segments s. The straight-line Gaussian solution is taken for description of each segment s in its first time step ΔT^{segm} of propagation within the time interval $<0; \Delta T^{segm}>$. In the subsequent time phases f of the segment s the meteorological conditions have to be considered more realistically. For this purposes a segmented Gaussian plume model (SGPM) is introduced (Hofman and Pecha, 2011). The model together with the algorithm proposed here is fully integrated into the environmental code HARP (HAzardous Radioactivity Propagation). The model SGPM is initiated from the first phase $f = 1$ of the straight-line propagation supposing the longitudinal dispersion is neglected. The analytical shape of the partial plume confined on interval $x \in <0; \Delta T^{segm}.\bar{u}>$ is described by expression (1). In the consecutive phases $f > 1$ the segment s is drifted according to the current changes of meteorological conditions. The further dispersion and deposition (e.g. $(s = 1; f = 1) \rightarrow (s = 1; f = 2)$ in Fig. 1) is simulated using the SGPM algorithm by means of a large number of elemental shifts driven by the new weather conditions (HARP, 2011). During each shift the activity depletion in the cloud due to dry and wet deposition and

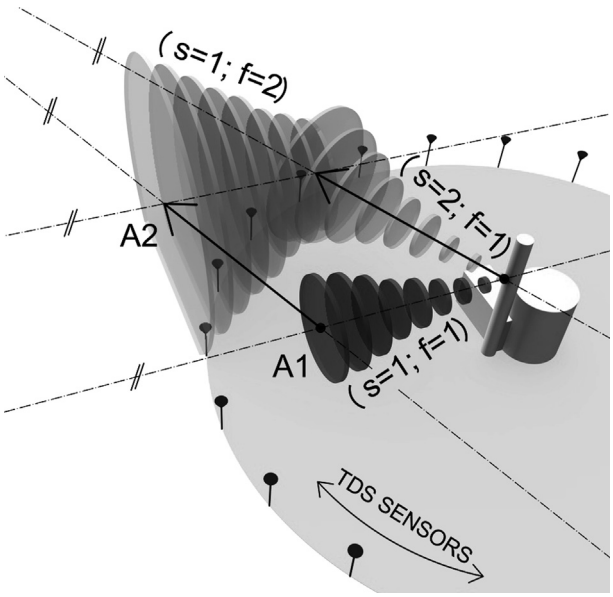

Fig. 1. The finite cloud propagation during stepwise changes of meteorological conditions. Weather changes observed/forecast for the point of release for a particular time step ΔT^{segm} are assumed to immediately impact the propagation of all previous segments in their corresponding phases.

radioactivity decay is assumed. A complicated scenario of a release time progress is synchronized with the available meteorological observations/forecasts.

The plume is assumed to be driven through the near vicinity by weather forecast given for the point of release. The time step of extents ΔT^{segm} should be selected according to accessibility of the meteorological data (one-hour or half an hour). During each time interval ΔT^{segm} a new set of the local observed/forecast meteorological data is assumed to be available in the nearest vicinity of the source. We can hardly expect to have the weather data in a fine spatial and time resolution (let us say for a few hundred metres from the source). We have adopted a certain intuitive subjective assumption for the plume spread in the nearest vicinity according to the sketch shown in Fig. 1. In this case the weather changes observed/forecast for the point of release for a particular time step ΔT^{segm} immediately and in the same way impact the propagation of all segments in their corresponding phases. The interval ΔT^{segm} of on-site meteorological measurements is typically from several minutes to one hour. Besides information related to the source of release we are also using a short-term meteorological forecast: 48 h forward on the spatial grid on an area of 200 × 200 km around the source of pollution. It enables us to connect the plume tracing at larger distances with the previous nearest-range analysis.

The initial straight-line plume propagation during the time step extent ΔT^{segm} is simulated by simplified solution of the diffusion equation in the form:

$$C^n(x,y,z) = \frac{A^n}{2\pi\cdot\sigma_y(x)\cdot\sigma_z(x)\cdot\bar{u}}\cdot\exp\left(-\frac{y^2}{2\sigma_y^2(x)}\right)\cdot\left[\exp\left(-\frac{\left(z-h_{ef}\right)^2}{2\sigma_z^2(x)}\right)+\exp\left(-\frac{\left(z+h_{ef}\right)^2}{2\sigma_z^2(x)}\right)+\exp\left(-\frac{\left(z-2H_{mix}+h_{ef}\right)^2}{2\sigma_z^2(x)}\right)+\eta_{JV}(x,z)\right]\cdot f_R^n(x)\cdot f_F^n(x)\cdot f_W^n(x) \quad (1)$$

$C^n(x,y,z)$ Specific activity of radionuclide n in spatial point (x,y,z) in (Bq m^{-3}); x – direction of spreading; y, z – horizontal and vertical coordinates

$\sigma_y(x)$, $\sigma_z(x)$ Horizontal and vertical dispersion coefficients at distance x from the source (m); expressed by empirical formulae

A^n Continuous release source strength of nuclide n (Bq s^{-1}); continuous and constant within the time interval ΔT^{segm}

$\bar{u}$ Mean advection velocity of the plume in direction x (m s^{-1})

h_{ef}, H_{mix} Effective height of the plume axis over the terrain (m), height of planetary mixing layer (m)

$\eta_{JV}(x,z)$ Effect of additional multiple reflections on ground and inversion layer/mixing height (for this near-field model hereafter ignored)

$f^n{}_R, f^n{}_F, f^n{}_W$ Plume depletion factors due to radioactive decay and dry and wet deposition. The latter two are dependent on the physical-chemical form (aerosol, organic, elemental) of nuclide n. The factors stand for the "source depletion" approach introduced into the classical straight-line Gaussian solution. The release source strength at distance x is depleted according to $A^n(x, y = 0, z = h_{ef}) = A^n(x = 0, y = 0, z = h_{ef})\cdot f^n{}_R(x)\cdot f^n{}_F(x)\cdot f^n{}_W(x)$ – more in (HARP, 2011).

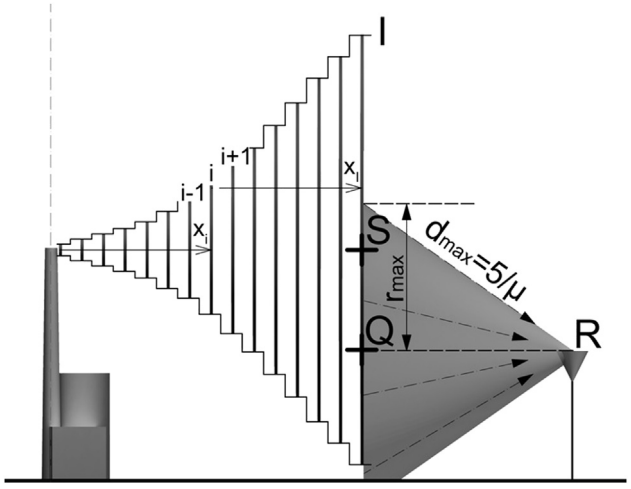

Fig. 2. Partitioning of continuous Gaussian shape into equivalent elliptical disc sequence i (i = 1,…,I). Irradiation of receptor R from the last disc I is illustrated.

The exponential terms in Equation (1) from left to right mean the basic diffusion growth of the plume, its reflection in the ground plane and its reflection from the top of mixing layer H_{mix}. The designed atmospheric dispersion model SGPM was compared with international codes COSYMA and RODOS (Pecha and Pechova, 2002; HARP, 2011). The documentation of the HARP system and other additional comparisons are described in detail in (HARP, 2011). The applicability of the straight-line propagation in the first hour of a release is limited on the near field areas inside the emergency planning zone around a nuclear facility up to 15–20 km. For a simple scenario the results are well comparable with the time consuming techniques based on Lagrangian particle dispersion models (eg. NAME III Bedwell et al., 2010; Armand et al., 2005) – see Section 6.

3. Proposition of the fast scheme for evaluation of external irradiation from radioactive cloud

We shall consider the physical quantity of the photon fluence which represents a number of monoenergetic γ photons with energy E_γ passing through a specific area. Transport of photons with energy E_γ from the source of emission to the receptors R will be described by the quantity of photon fluence rate $\Phi(E_\gamma, R)$ in units (m^{-2} s^{-1}). External exposure from the finite plume can be estimated when applying traditional methods based on three-dimensional integration over the cloud (e.g. ADMS4, 2009) or on specially constructed three-dimensional columned space divided into many finite grid cells (e.g. Wang et al., 2004). Photon fluence rate at a receptor point R on the terrain from the whole plume volume V_{plume} emitting monoenergetic γ-photons of energy E_γ is calculated according to the three-dimensional integration given by Equation (2).

$$\Phi_{total}(E_\gamma,R) = \iiint_{V_{plume}} \frac{f^n(E_\gamma)\cdot C^n(x,y,z)\cdot B(E_\gamma,\mu(E_\gamma)\cdot d)\cdot\exp(-\mu(E_\gamma)\cdot d)}{4\pi d^2}\mathrm{d}V \quad (2)$$

Table 1
Photon fluence rate induced by a plume as a function of Δx from Equation (3b). Responses on sensors TST01 and TST02 just T_{minute} after the start of continuous release of ^{133}Xe with source strength from Table 4. Duration of release is 1 h.

Sensor[b]	T_{minute} (min)	Photon fluence rate (m^{-2} s^{-1})[a]		
		$\Delta x = 1$ m	$\Delta x = 10$ m	$\Delta x = 50$ m
TST01	5	1.568E+11	1.452E+11	8.180E+10
TST01	6	4.745E+11	4.786E+11	4.727E+11
TST01	≥8[c]	5.485E+11	5.483E+11	5.373E+11
TST02	20	1.101E+11	1.035E+11	1.259E+11
TST02	≥23[c]	2.813E+11	2.760E+11	2.469E+11
Relative time of computation up to 1 h of the cloud propagation		1.0	~0.10	~0.02

[a] Continuous release of radionuclide ^{133}Xe with the source strength 2.28E+14 Bq s^{-1}.
[b] TST01, TST02 are located at 400 m and 1500 m respectively from the source.
[c] Equilibrium values of photon fluence rate are constant up to the end of the continuous release.

where $\mu(E_\gamma)$ is the linear attenuation factor (m^{-1}), d denotes the distance between the receptor point R and the plume elemental volume dV. $B(E_\gamma,\mu(E_\gamma)\cdot d)$ stands for the build-up factor. We use its linear form $B(E_\gamma,\mu\cdot d) = 1 + k\cdot\mu\cdot d$. Here $k = (\mu - \mu_a)/\mu_a$, μ_a stands for the linear energy absorption coefficient (m^{-1}). Both coefficients are related to the monoenergetic photons with energy E_γ. Comparison of the linear form with the alternative Berger's formula can be found in literature, e.g. in Overcamp (2007). Specifically, we can assume the monoenergetic γ-photons emitted by the radionuclide n. The value $f^n(E_\gamma)$ is the branching ratio for radionuclide n to the specified energy E_γ. Activity concentration C^n of radionuclide n in the air is given by the analytic Equation (1).

Continuous and constant release in direction of axis x with average velocity $\overline{u}$ is partitioned into an equivalent number of elliptic discs according to Fig. 2. The thickness of the discs Δx was tested for the optimal choice (see conclusion in Table 1 below). The centre of the disc i reaches the position $x_i = (i - 1/2) \times \Delta x$ in $x_i/\overline{u}$ seconds. A discrete technique is introduced when the model parameters are averaged within interval Δx on the disc i. Distribution of the activity concentration in the disc i on the plane $x = x_i$ (it means the average value on Δx) is driven according to the straight-line Equation (1) where the corresponding averaged sources of irradiation that lie within a distance of $5/\mu(E_\gamma)$ from the receptor R. The integration boundary (see also the integration circle in Fig. 3) is formed by intersection of the cone (receptor R is in the cone vertex) and the plane of the newest disc I. Only the points located inside are assumed to contribute to the fluence rate at R. This markedly accelerates the computational speed and improves the capability of the assimilation procedures to run successfully in real time mode. It can, for a near-field problem, serve as an effective alternative to computationally expensive traditional methods based on full 3-D integration techniques (Raza et al., 2001).

A substantial performance improvement makes the $5/\mu(E_\gamma)$ approach the first choice for its application during nuclear emergency situations (Wang et al., 2004). Minor differences from the traditional methods of coarse 3-D integration are referred to here for a broad range of input model parameters (stability classes, axial distances, source term characteristics etc.). The partial results of spatial progression for stability classes F and D are given in Fig. 5 below. A comparison benchmark of the results with several European codes is presented in Section 6.2.

4. Replacement of traditional 3-D integration by stepwise 2-D computational scheme

4.1. Formulation of the stepwise 2-D computational approach

External irradiation from the plume section on interval $<x_i - \Delta x/2; x_i + \Delta x/2>$ is substituted by an equivalent effect of a disc of thickness Δx with averaged model parameters on $<x_i - \Delta x/2; x_i + \Delta x/2>$. Let us analyse the contribution to the fluence rate at the receptor R from irradiation with monoenergetic photons having energy E_γ from the elliptical disc I. A lateral view of the partitioned plume propagation is demonstrated in Fig. 2. The same situation is outlined in the front view in Fig. 3. The boundary of the integration region lying in the plane of disc I is based on $5/\mu(E_\gamma)$ approximation (bold dashed line composed of the part of the circle above ground with a radius of r_{max} and with its centre in the point Q). For r_{max} the relationship $r_{max}^2 = (5/\mu(E_\gamma))^2 - [x(R) - x(Q)]^2$ holds true. The points S and Q are lying in the plane of disc I (S is its centre, the abscissa RQ is perpendicular to the plane). Contribution of the disc I with unit thickness $\Delta x = 1$ m to the photon fluence rate at receptor R is given by:

$$\Phi^{\Delta x=1}(E_\gamma, R, I, x_I) = \frac{1}{4\pi}\int_{r=0}^{r_{max}}\int_{\varphi=0}^{2\pi}\frac{f^n(E_\gamma)C^I(x_I;r,\varphi)\cdot B(E_\gamma,\mu(E_\gamma)\cdot d)\cdot\exp(-\mu(E_\gamma)\cdot d)}{d^2} r d\varphi dr \quad (3a)$$

disc parameters are inserted (e.g. x_i, $\sigma_y(x_i)$, $\sigma_z(x_i)$, depletion factors $f_R^n(x_i)\cdot f_F^n(x_i)\cdot f_W^n(x_i)$ etc.).

The $5/\mu(E_\gamma)$ method (Wang et al., 2004) (generally $m/\mu(E_\gamma)$ method – the values m = 5,10,15 were tested) imposes an integration limit up to d_{max} and indicates as significant only those

The contribution from the disc I, which in general has a thickness of Δx, can be roughly expressed as:

$$\Phi(E_\gamma, R, I) = \Delta x\cdot\Phi^{\Delta x=1}(E_\gamma, R, I, x_I) \quad (3b)$$

Table 2
Model comparison for effective cloudshine dose rates for adults (m Sv s^{-1}) at 3 sensors along the plume centre line.

	NAME III[a]	ADMS[a]	PC CREAM[a]	HARP		
				Hosker (av. 24 h)	Hosker (no averaging)	KFK
1 km downwind	$2.3\cdot10^{-09}$	$2.1\cdot10^{-09}$	$3.2\cdot10^{-09}$	$2.52\cdot10^{-09}$	$8.51\cdot10^{-09}$	$3.44\cdot10^{-09}$
2 km downwind	$1.1\cdot10^{-09}$	$8.2\cdot10^{-10}$	$1.3\cdot10^{-09}$	$1.04\cdot10^{-09}$	$4.07\cdot10^{-09}$	$1.47\cdot10^{-09}$
5 km downwind	$5.1\cdot10^{-10}$	$2.2\cdot10^{-10}$	$3.5\cdot10^{-10}$	$3.17\cdot10^{-10}$	$1.35\cdot10^{-09}$	$3.79\cdot10^{-10}$

[a] The values selected from Bedwell et al. (2010).

Table 3
Comparison of calculated dose rates with tabulated DCFs.

Nuclide	$\overline{E}^n$ (MeV)	$\omega(\overline{E}^n)$	$5/\mu$ (m)	Dose rate (Sv s^{-1}/(Bq/m^3))	DCF (ICRP 74, 1996) (Sv s^{-1}/(Bq/m^3))
^{41}Ar	1.293	0.735	6.84E+02	5.47E-14 5.93E-14[a]	6.50E-14
^{131}I	3.625E-01	0.666	3.56E+02	1.18E-14 1.545E-14[a,b]	1.78E-14
^{133}Xe	5.230E-02	0.541	2.01E+02	1.62E-15	1.56E-15

[a] Higher integration limit up to $10/\mu$.
[b] Linear formula for build-up factor.

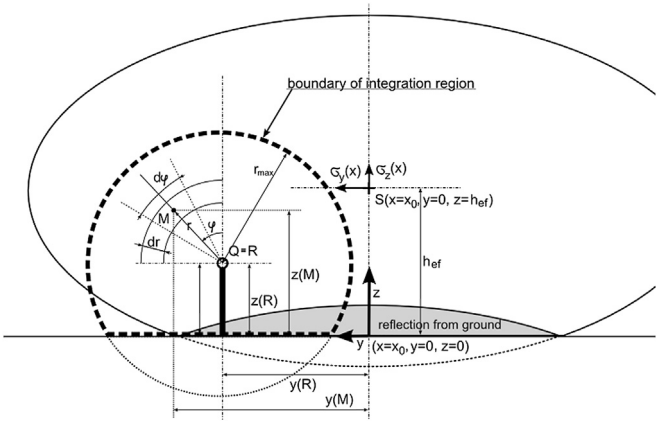

Fig. 3. (Coupled with Fig. 2): Frontal view from the receptor point R to the elliptical disc I and circular integration region (bold dashed line).

Referring to Fig. 3, the value of d is distance between points $R(x(R),y(R),z(R))$ and $M(x(S), y(M), z(M))$; $d^2 = (x(S) - x(R))^2 + (y(M) - y(R))^2 + (z(M) - z(R))^2$; $x(S) = x_I = (I-1/2) \times \Delta x$ is the distance of the centre of the disc I from the release point; $y(M) = y(R) + r \times \sin(\varphi)$; $z(M) = z(R) + r \times \cos(\varphi)$. The equivalent specific source strength $C^I(x_I, y, z)$ of emitted monoenergetic photons in the disc I is expressed using C^n from Equation (1) multiplied by branching ratio $f^n(E_\gamma)$. Valid values of coordinate z should be positive, dispersion coefficients and depletion factors are calculated for position x_I (it means for a time of $x_I/\overline{u}$ s) and are dependent on the physical–chemical form of the respective radionuclide.

An equivalent source strength for the disc I includes source depletion model and substitutes the original discharge from Equation (1) according to $A(x_I, y = 0, z = h_{ef}) = A(x = 0, y = 0, z = h_{ef}) \cdot f_R(x_I) \cdot f_F(x_I) \cdot f_W(x_I)$. During computation the values of photon fluence rates are gradually stored into the array $F(1{:}N_{sens}, 1{:}I_{total})$. Here N_{sens} means the number of receptors being simultaneously taken into account, and I_{total} stands for the total number of discs with thickness Δx of the plume separation (I_{total} is in order of 10^3). The total fluence rates, total fluencies and the corresponding total cloudshine doses/dose rates are generated by processing of the array values in the particular time steps $x_i/\overline{u}$, $i = 1, \ldots, I_{total}$.

4.2. Selecting the computational grid size in practice

The proposed stepwise numerical scheme is shown in Fig. 2. The precision of calculations on the one hand and computational time on the other hand depend on the choice of the disc thickness Δx entering the Equation (3). Thickness of the discs was tested for selected values $\Delta x = 1$ m, 10 m, 50 m (see the conclusions in Table 1 below). Table 1 demonstrates the importance of an effective choice of the thickness value Δx. Fine resolution $\Delta x = 1$ m leads to about 50 times prolongation of the calculations with respect to the rough grid $\Delta x = 50$ m. The latter one gives some differences, mainly at locations near the source of pollution. Practically all computations were performed with $\Delta x = 10$ m proposed here as an optimum compromise between the precision and speed of computation. The affirmation should be valid for all nuclides (^{133}Xe has almost the lowest $\overline{E}^{Xe133}$ (see Table 4) and does have the lowest mean free path in air).

However, the equilibrium values can apparently be generated even with rough grid sizes. The values of the photon fluence rates at certain positions can reach their equilibrium values during a long-lasting release and remain constant for the remaining progress of the plume (e.g. see constant part of the courses in Fig. 4 left).

5. Formulation of the fast computational procedure in the initial phase of the plume propagation

The subsequent post-processing of the array F described above provides a sufficient approximation to the basic solution described by Equation (3). Fig. 2 shows the scheme for the fragmentation of the plume shape into the consecutive virtual elliptical discs. The first segment of propagation during the time steps ΔT^{segm} is assumed to be described by the corresponding part of straight-line Gaussian formula. In the following text we shall examine a basic task, namely a linear drifting of the segment in its first phase $f = 1$ (described in Figs. 1 and 2) and generation of responses in a large net of sensors. The analysis for the first phase $f = 1$ is of essential significance because it comprises the teledosimetric ring of sensors (TDS) on the fence of the nuclear power plant (roughly 25 sensors at distances of approximately 500 m from the hypothetical source of pollution). The ring plays the decisive role in re-estimation of the source term of release and some other model parameters on the basis of assimilation with incoming terrain measurements.

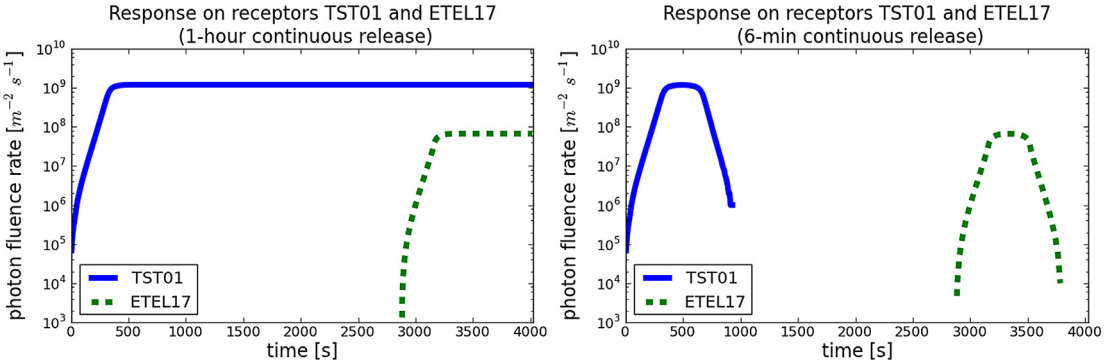

Fig. 4. Time evolution of responses on sensors TST01 and ETEL17 from the beginning of release with continuous source strength 9.0E+14 Bq/h of ^{131}I. Left: Continuous one-hour spreading. Right: Spread of the shorter plume of 6 min duration.

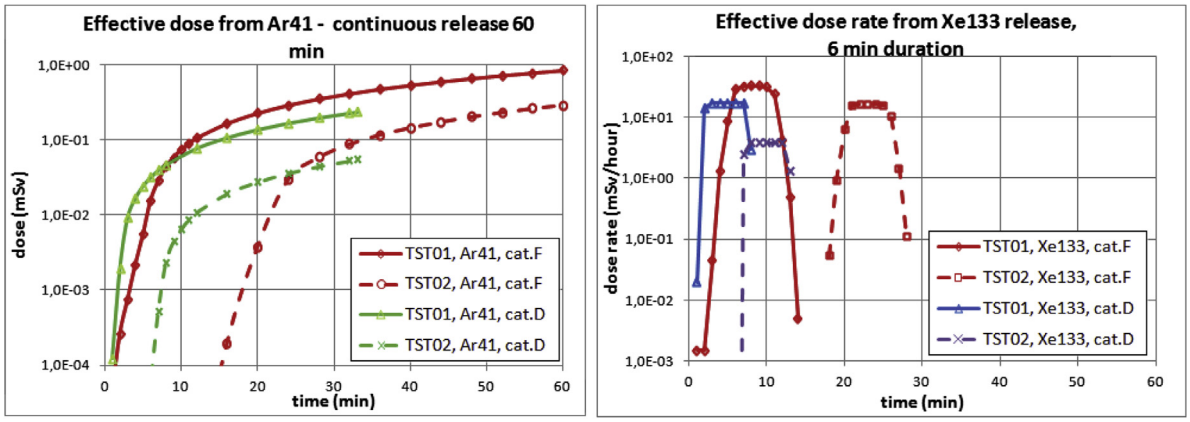

Fig. 5. Time evolution of the effective individual cloudshine doses at positions of sensors TST01 and TST02 (400 m and 4000 m respectively in the direction of the plume propagation). Continuous 1-h release of ^{41}Ar with strength 3.33E+11 Bq s^{-1} (left). Short 6-min continuous release of ^{133}Xe with strength 2.78E+14 Bq s^{-1} (right).

The front of the plume is determined by the position of the latest disc I of the bundle of discs which corresponds to the time of spreading $t_I = I \times \Delta x/\bar{u}$. Recurrent formulae for processing an array of fluencies can be derived when distinguishing between two situations.

5.1. The continuous release with steady state discharge rate of admixtures persists

Let us assume the front of the plume has reached the position of the disc I, and propagation to the $I+1$ disc is in progress. Contribution of each elemental disc $i = 1, \ldots, I$ to the fluence rate $\Phi(E_\gamma, R, i)$ at receptor R was calculated in the previous steps and stored in the array F. The new contribution $\Phi(E_\gamma, R, I+1)$ of the disc $I+1$ is calculated using integration (3). The recurrent formula for over all fluence rate at receptor R can be formally rewritten as:

$$\Phi(E_\gamma, R, i = 1, \ldots, I+1) = \Phi(E_\gamma, R, i = 1, \ldots, I) + \Phi(E_\gamma, R, I+1)$$
$$\text{where} \quad \Phi(E_\gamma, R, i = 1, \ldots, I) = \sum_{i=1}^{i=I} \Phi(E_\gamma, R, i) \tag{4}$$

Then, the only computation effort is to evaluate 2-D integration of the latest disc $I+1$. Analogously, the recurrent formula for the entire photon fluence at receptor R from the same beginning of the release is given by:

$$\Psi(E_\gamma, R, i = 1, \ldots, I+1) = \Psi(E_\gamma, R, i = 1, \ldots, I) + \sum_{i=1}^{i=I+1} \Delta t_i \cdot \Phi(E_\gamma, R, i)$$
$$\text{where} \quad \Psi(E_\gamma, R, i = 1, \ldots, I) = \sum_{i=1}^{i=I} \left[(I+1-i) \cdot \Delta t_i \cdot \Phi(E_\gamma, R, i)\right] \tag{5}$$

$$\Delta t_i = \Delta t = \Delta x/\bar{u} \text{seconds}$$

5.2. Release terminated, propagation continues

Let the front of the plume has reached the position of the disc I just at the moment when the release has terminated. Propagation continues to the disc positions $I+1, I+2, \ldots, I+j$. Fluence rate for the new front cloud position at disc $I+j+1$ is calculated from the previous position $I+j$ according to the recurrent formula:

$$\Phi(E_\gamma, R, i = j+1, \ldots, I+j+1) = \Phi(E_\gamma, R, i = j, \ldots, I+j) + \Phi(E_\gamma, R, I+j+1) - \Phi(E_\gamma, R, j+1) \tag{6}$$

Hence, the contribution from the leftmost disc of a parcel is skipped and the fluence $\Phi(E_\gamma, R, I+j+1)$ induced by the new rightmost disc $I+j+1$ is calculated according to 2-D integration (3). Similar considerations lead to the recurrent expression for the total fluence Ψ:

$$\Psi(E_\gamma, R, i = 1, \ldots, I+j+1) = \Psi(E_\gamma, R, i = 1, \ldots, I+j) + \sum_{i=j+1}^{i=I+j+1} \Delta t_i \cdot \Phi(E_\gamma, R, i) \tag{7}$$

Note: As mentioned in Chapter 2, the subsequent phases $f > 1$ are simulated using the SGPM algorithm which performs a large number of elemental shifts driven by the new weather conditions. Following Fig. 1, the plume segment shift $(s = 1; f = 1) \rightarrow (s = 1; f = 2)$ also proceeds generally in the lateral direction. The concept of recurrent expressions cannot be applied here. We can use the dispersion solution just after the shifts $f \rightarrow f+1$. The immediate values of the fluence rates related to the new position of the plume in the end of the phase $f+1$ can be easily calculated using the proposed stepwise 2-D computational scheme. Nevertheless, for the later phases the formula for semi-infinite cloud is usually accepted (depending on vertical homogenisation of the concentration). The direct utilisation of the 3-D integration can be taken into consideration for some individual areas having a special significance.

5.3. An illustrative example of application of the recurrent formulae

We assume the release of radionuclide ^{131}I with $E_\gamma = 0{,}3625$ MeV (γ – yield is taken to be 100%, linear attenuation coefficient $\mu = 1.41$E-02 (m^{-1}), linear energy absorption coefficient

Table 4
Hypothetical source term and averaged photon energies according to Equation (10).

Radionuclide	^{41}Ar	^{88}Kr	^{131}I	^{132}I	^{135}I	^{132}Te	^{133}Xe	^{135}Xe	^{134}Cs	^{137}Cs
Activity release (Bq/h)	1.2E+15	1.2E+17	9.0E+14	2.2E+15	2.2E+15	5.5E+13	8.2E+17	6.6E+17	3.2E+13	7.9E+13
$\bar{E}^n$ – Equation (10) in MeV	1.293	1.348	0.362	0.762	1.192	0.136	0.052	0.250	0.695	0.614
Half-time of decay	1.8 h	2.8 h	8.01 d	2.3 h	6.6 h	78.6 h	5.2 d	9.1 h	2.06 y	30.0 y

$\mu_a = 3.30969E\text{-}03\ (m^{-1})$ (interpolated value). Mean free path values are $1/\mu = 7.12E{+}01$ m, $5/\mu = 3.56E{+}02$ m, and $10/\mu = 7.12E{+}02$ m. Time evolution of the fluencies/fluence rates from 1 h continuous activity release 9.0E+14 Bq/hour of ^{131}I (selected from Table 4) is simulated. Effective height h_{ef} of the release is 45 m, Pasquill categories of atmospheric stability F are examined (wind velocity at 10 m height $u_{10} = 1.0\ m\ s^{-1}$). Short term meteorological forecast is for 20080111_18 (January 11th, 2008, 18.00 CET), and the wind blows in the direction of 273 deg.

Time evolution of the fluencies/fluence rates for category F for sensors TST01 and ETEL17 (roughly 400 m and 4000 m respectively in direction of the plume propagation) is simulated in Fig. 4. Long continuous release of ^{131}I having duration 1 h is examined by Equations (4) and (5) (see left part). The right side of Fig. 4 concerns the spreading of shorter plume of 6 min duration. Within the 6 min interval the propagation is treated by Equations (4) and (5). After that the continuous release stops and the cloud is torn away the source. The fluence rates and fluencies are then governed by Equations (6) and (7).

6. Tests and comparisons of results

The proposed algorithm is tested for various release dynamics and model parameters. The method m/μ was examined for $m = 5$ and $m = 10$ but the differences are small (a few per cent). The calculations for $m = 5$ are more than three times faster in comparison with $m = 10$. Verification of the numerical integration algorithm expressed in Equation (3) is accomplished in Appendix A. The numerical results are compared with the analytical solution of Equation (3) for a special case without absorption ($\mu = 0$) and build-up factor $B = 1$ (a simplified experiment – "irradiation in vacuum"). Convergence to the semi-infinite cloud solution is examined in Section 6.3.

6.1. Derivation of the external irradiation dose from the photon fluencies

At first we shall formulate the relationship between the photon fluency/fluency rate and the individual effective dose/dose rate of external irradiation from the cloud. The irradiation dose rate at the receptor R is denoted by $H(E_\gamma,R,i = 1,\ldots,I)$ (Gy s^{-1}). It represents the irradiation from monoenergetic photons with energy E_γ emitted from the whole plume (with the disc I in the front). It can be calculated from the fluence rates (see Equations (4) or (6)) according to:

$$H(E_\gamma, R, i = 1,\ldots,I) = \frac{\omega \cdot K \cdot \mu_a \cdot E_\gamma}{\rho} \cdot \Phi(E_\gamma, R, i = 1,\ldots,I) \qquad (8)$$

Conversion factor $K = 1.6 \cdot E10^{-13}$ Gy kg Mev^{-1}; $\omega = 1.11$ is a ratio of the absorbed dose in tissue to the absorbed dose in air (more precise energy dependence is mentioned in Table 3), and the air density $\rho = 1.293$ kg m^{-3}. The other quantities for the release of radionuclide ^{131}I were described in the beginning of Section 5.3. Equation (8) stands for absorbed doses expressed in grays. Common practice in the radiation protection field is to multiply the absorbed doses by relative biological effectiveness factor F_q which accounts for different biological damage with regards to different types of ionizing radiation. The corresponding radiological quantity is expressed in Sv (sieverts), where $F_q = 1$ for photons. Therefore, we shall express doses in the following text and graphs in units of Sv.

The application stemming from of Equation (8) is given in Fig. 5. The influence of the changing meteorological conditions for Pasquill stability categories F and D ($u_{10} = 1.0\ m\ s^{-1}$ and $3.0\ m\ s^{-1}$ respectively) is examined for two nuclides with different gamma energy levels. ^{41}Ar has high photon energy and long mean free path, while ^{133}Xe has low photon energy and shorter mean free path (see Table 3). The source strengths of both nuclides correspond to the values in Table 4. The dispersion formulae KFK-Jülich for rough terrain are used.

6.2. Confrontation of the cloudshine doses generated nearby the source

Computer simulations are critical especially in high-consequence systems that can hardly ever be tested in a fully representative environment. Plausibility of simulations can be tested also on consensus of the computational simulations with the physical nature of the problem. An example of such partial test is in Fig. 6. Expected progress of both curves is confirmed. The proposed algorithm covers realistically the ring of teledosimetric sensors located about 500 m around the source.

In the following text we shall carry out the convention comparison benchmark based on confrontation of the results with several well-established international environmental codes. In the article (Bedwell et al., 2010) a hypothetical scenario of ^{85}Kr discharge with intensity 1.0×10^{10} Bq s^{-1} over a 24 h period is analysed. Other characteristics were used: release height of 10 m, constant wind direction with a speed of 5 m s^{-1}, a boundary layer depth of 800 m, heat flux of 0 W m^{-2}, representative Pasquill stability category D, no rain, and terrain roughness of 0.3 m. Three receptor points are considered at 1, 2, and 5 km along the plume centre line. The effective cloud gamma dose rates are to be estimated, averaged over 24 h after the start of release. Monoenergetic photons having energy of 0.5300 MeV with yield $4.340 \cdot 10^{-3}$ per decay are assumed according to RadDecay (1996). We have taken Table 1 from Bedwell et al. (2010) related to the three significant European computer codes NAME III (Lagrangian particle-puff trajectory model), ADMS4 (3-D integration for calculation of photon fluence, dispersion described by the new generation of Gaussian plume model based on advanced parameterisation of the boundary layer structure) and PC CREAM (Smith and Simmonds, 2008) (Gaussian quadrature for 3-D numerical integration, dispersion using standard Gaussian plume model based on classical single parameter Pasquille–Gifford stability categories). The original comparison from Bedwell et al. (2010) was extended by our results (see Table 2). The outputs were generated by the environmental code HARP (HARP, 2011) to which the new proposed algorithm for cloudshine doses estimation is fully integrated.

The HARP system is designed for sensitivity analysis and assessment of the "worst case" accidental scenarios. User-friendly environment enables quick examination of variability for the

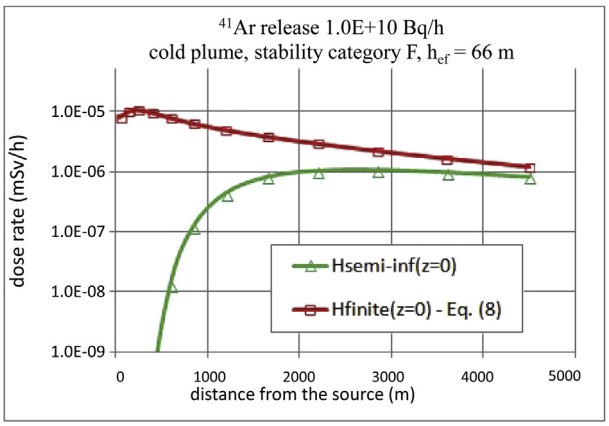

Fig. 6. Comparison of the finite cloud dose rates H_{finite} ($z = 0$) calculated according to the proposed model using Equation (8) with the semi-infinite approach $H_{semi\text{-}inf}$ ($z = 0$). $E_\gamma = 1.2936$ MeV for radionuclide ^{41}Ar (γ – yield is 99.1%).

input model parameters. Three alternative formulae for horizontal dispersion σ_y are used to obtain the results shown in Table 2. Hosker dispersion formulae are derived for smooth terrain using a sampling time of 10 min. Rough averaging of σ_y over a period of 24 h was done using the recommendations given in (Hanna et al., 1982) in order to fulfill the comparison requirements given above. For illustration, results for σ_y related to the original sampling time of 10 min are also given in Table 2. The values have evident physical meaning as instantaneous (un-averaged) dose rates. The results for KFK-Jülich dispersion model presented in the last column in Table 2 can illustrate the sensitivity of the results using the option of the alternative dispersion formulae for smooth versus rough terrain (KFK formulae are predetermined for rough terrain of the Central European type). The results in Table 2 generated by the HARP system in near distances from the source of pollution are well comparable with the established international codes.

6.3. Verifying the convergence of the external γ-exposure to the semi-infinite cloud solution

The dose conversion factor (DCF) for external exposure of a person submerged in the semi-infinite cloud with uniform specific radioactivity of 1 Bq m^{-3} represents a dose rate in units (Sv s^{-1} Bq^{-1} m^3). The recommended factors are selected from (ICRP 74, 1996). The proposed algorithm was adjusted for these special calculations. The value of radioactivity concentration C in Equation (3) in ambient air was assumed to be 1 Bq m^{-3} everywhere in any disc from the plume segmentation according to Fig. 2. Three radionuclides with markedly different average photon energies were considered according to Table 3. Segment thickness Δx is 10 m (see. Equation (3)), Berger's formula for build-up factor is used and the integration limit is $5/\mu$ (see Fig. 2). Here ω is the ratio of effective dose to air dose for the respective energy for isotropic irradiation geometry (ICRP 74, 1996).

We can hardly expect an excellent agreement of our computations with a detailed DCF determination based on Monte Carlo calculations with a human phantom model. Photon transport mechanisms are simplified using empirical formulae (build-up factors, ratio ω). However, Table 3 shows good agreement of the proposed algorithm with ICRP recommendations. At the same time, the results are well comparable with findings of other authors, e.g. (Wang et al., 2004) where 3-D integration is substituted by a three-dimensional columned space subdivision on many finite grid cells, or (Armand et al., 2005) where a gamma exposure rate is simulated with 3-D Lagrangian particle model SPRAY with the post-processor tool CLOUD_SHINE.

The results shown in Table 3 are assumed to provide sophisticated particular evidence of proper functionality of the proposed technique.

7. Accounting for multiple nuclide group

We assume the multiple photons p emitted with different energies $E^n{}_p$ from radionuclide n which have noticeable yields $f^n{}_p$ (e.g. greater than 0.001). Following Equation (8) the general expression for dose rate (Sv s^{-1}) from the multiple nuclides/multiple photons case can be rewritten as:

$$H(R,i=1,\ldots,I)=\sum_{(n)}H^n(R,i=1,\ldots,I)=\frac{\omega\cdot K}{\rho}\sum_{(n)}\sum_{(p)}\mu_a\left(E_p^n\right)\cdot f_p^n\cdot E_p^n\cdot\Phi\left(E_p^n,R,i=1,\ldots,I\right) \tag{9}$$

The corresponding dose in Sv can be calculated when substituting the fluence rate Φ by the entire photon fluence Ψ expressed by Equation (5) or (7).

7.1. Averaging photon energies for each nuclide

Reduction of the computational load can be achieved by averaging the photon energies for the nuclide n according to:

$$\overline{E}^n=\sum_{(p)}f_p^n\cdot E_p^n/F^n;\quad F^n=\sum_{(p)}f_p^n \tag{10}$$

The subsequent simplified formulation for the dose rate is:

$$H(R,i=1,\ldots,I)=\sum_{(n)}H^n(R,i=1,\ldots,I)=\frac{\omega\cdot K}{\rho}\sum_{(n)}\mu_a\left(\overline{E}^n\right)\cdot\overline{E}^n\cdot F^n\cdot\Phi\left(\overline{E}^n,R,i=1,\ldots,I\right) \tag{11}$$

We have examined a hypothetical release of nuclide mixture illustrated in Table 4. Dependency of physical coefficients on photon energy (for linear and mass attenuation coefficients, constants in build-up factor formulae, etc.) is interpolated from discrete values prepared in Pechova (2012).

The outputs presented here are results of the model simulations using the proposed technique just at the points of existing fixed monitoring networks. The bilinear interpolation technique is used for determination of the values in an arbitrary location.

Part of the results generated according to the simplified scheme (11) for sensor TST01 is demonstrated for each nuclide in Fig. 7. The radionuclide mixture is discharged into the atmosphere with a category stability class F. The effective height of release is $h^{ef}=45$ m, and wind speed at a height of 10 m is $u_{10}=1.0$ m s^{-1}. Due to dependency of H in Equation (11) on energy, the shape of curves for photon fluence rates (left) somewhat differs from the corresponding dose rates (right). The calculations for all nuclides and for all sensors are running in one stroke. A significant outcome is achieved by computation effectiveness, when the complete run for all nuclides and all sensors lasts about 90 s on a PC with a standard, common configuration.

7.2. Substitution of multi-nuclide approach to multi-group scheme

Equation (3) is formulated for simplified case of a nuclide emitting one photon with average energy E_γ per decay. Some nuclides have a rather wide spectrum of emitted photons. We can expect a certain inaccuracy to be introduced to the results when using computational schemes (10) and (11) with only average energy. The straightforward solution offers a detailed scheme given by Equation (9). But it could cause a huge escalation of computational load and the main goal of a real time analysis may not be achievable.

An alternative method is proposed here with the goal of making further calculations more accurate and at the same time sufficiently fast for a large group of nuclides discharged into the atmosphere. The whole range of possible photon energy levels is partitioned into G energetic groups: $G=24$ and alternatively $G=8$ were selected according to Pechova (2012), RadDecay (1996). Probability and emitted energy values were extracted for each photon p of a cascade belonging to each nuclide from the nuclide mixture. Linear total gamma attenuation coefficients μ and linear gamma energy-absorption coefficients μ_a are interpolated on the basis of the same energetic separation. Let $^nE^g{}_p$ stands for energy of each photon p emitted by the nuclide n having energy belonging to the group g with the yield of $^nf^g{}_p$. The mean energy $\overline{E}^g(x_I)$ averaged over all photons emitted to the energy interval g from all radionuclides n at downwind distance x_I can be found using the "source

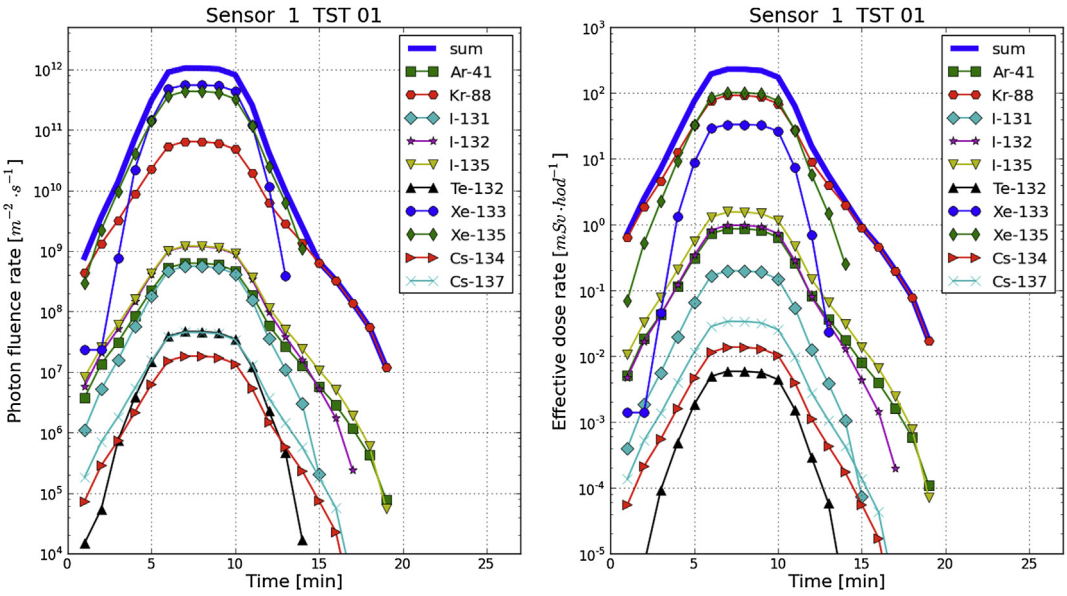

Fig. 7. Response of sensor TST01 in the photon fluence rate (left) and dose rate (right) on a short release of 6-min duration. Sensor TST01 is located at a distance of about 400 m from the source, roughly in the direction of the plume propagation. Multi-nuclide source term is defined according to Table 4.

depletion" approach introduced in Equation (1): $A^n(x_I,\ y\ =\ 0,\ z\ =\ h_{ef}) = A^n(x = 0, y = 0, z = h_{ef})\cdot f^n{}_R(x_I)\cdot f^n{}_F(x_I)\cdot f^n{}_W(x_I)$. The values of $\overline{E}^g(x_I)$ are determined according to Equation (12). Depletion factors for dry and wet deposition $f^n{}_F(x_I)$ and $f^n{}_W(x_I)$ have to be distinguished according to the physical–chemical forms of radionuclides, landuse characteristics of the terrain and precipitation intensity – more details can be found in the documentation of the HARP product (HARP, 2011).

$$\overline{E}^g(x_I)\ =\ \sum_{n=1}^{N} A^n(x_I)\cdot\overline{E}^g_n\cdot F^g_n \Big/ \sum_{n=1}^{N} A^n(x_I)F^g_n;\quad \overline{E}^g_n\ =\ \sum_{(p(n))}{}^{nAp(n)A}E^g_p \cdot{}^{nAp(n)A}f^g_p;\quad F^g_n\ =\ \sum_{(p(n))}{}^{nAp(n)A}f^g_p \tag{12}$$

The denominator in Equation (12) represents the total number of photons emitted in disc I per second from all nuclides belonging to the group g. Now we introduce an expression for the photon fluence rate from the total number of photons emitted from all nuclides belonging to the energetic group g. After separation of the nuclide part and the spatial integration part, Equation (3) can be rewritten as:

$$\Phi^g\left(\overline{E}^g(x_I), R, I\right)\ =\ \mathrm{SUM}(x_I;g)\cdot\mathrm{INTEG}(x_I;R,g) \tag{13}$$

$$\mathrm{SUM}(x_1;g)\ =\ \sum_{(n)} A^n\cdot f^n_R(x_I)\cdot f^n_F(x_I)\cdot f^n_W(x_I)F^g_n$$

$$\mathrm{DISPER}(x_I;y = y(r,\varphi),z = z(r,\varphi))\ =\ \frac{1}{2\pi\cdot\sigma_y(x_I)\cdot\sigma_z(x_I)\cdot\overline{u}} \cdot\exp\left(-\frac{y^2}{2\sigma^2_y(x_I)}\right)\left[\exp\left(-\frac{\left(z-h_{ef}\right)^2}{2\sigma^2_z(x_I)}\right)+\exp\left(-\frac{\left(z+h_{ef}\right)^2}{2\sigma^2_z(x_I)}\right) +\exp\left(-\frac{\left(z-2H_{mix}+h_{ef}\right)^2}{2\sigma^2_z(x_I)}\right)+\eta_{JV}(z)\right]$$

Where INTEG is expressed in analogy with Equation (1), but specifically stands for distribution of the fluence rate of photons at receptor point R from all nuclides contributing to the energetic group g. The resulting values are given by summing over all energetic groups g. It substitutes the former procedure based on the cycle over all nuclides.

7.3. Performance of multi-group approximation

The main achievement of the outlined technique illustrated above is the fact, that the time consuming integration INTEG is nuclide independent. Earlier repetitive estimation for each nuclide (or in detail for each photon p emitted by a nuclide described by Equation (9)) can be avoided. This alternative scheme is assumed to accelerate calculations for the scenarios with a large number (several tens) of discharged nuclides. For a medium group of 10 nuclides from Table 4, the former calculations according to expression (11) (run1) are compared with the multi-group approach for a fine resolution into 24 energetic groups (run2) and a rough resolution into 8 groups (run3). The computation of run3 is about three times faster than run2 and about 2.5 times faster than run1. The substantial advantage will be brought for large nuclide

$$\mathrm{INTEG}(x_I;R,g)\ =\ \frac{\Delta x}{4\pi}\int_{r=0}^{r_{\max}}\int_{\varphi=0}^{2\pi}\frac{\mathrm{DISPER}(x_I;y,z)\cdot B\left(\overline{E}^g(x_I),\mu\left(\overline{E}^g(x_I)\right)\cdot d\right)\cdot\exp\left(-\mu\left(\overline{E}^g(x_I)\right)\cdot d\right)}{d^2}\mathrm{rd}\varphi\mathrm{d}r$$

groups. The computational time of run1 is expected to be linearly proportional to the nuclide count while the computational time of the multi-group approach will be more or less constant, regardless of the increasing count of nuclides. As for dose estimates, for the medium nuclide group from Table 4, a small mutual differences have occurred. More systematic examination should be carried out for scenarios with a large number of released nuclides. Grouping of the gamma rays according to energies was extended (Pechova, 2012) for additional nuclides belonging to an extensive release of a hypothetical radiation accident. A hypothetical severe accident with the training source term ST2 selected from the RODOS system has been now recalculated using the proposed multigroup scheme. The scenario is initiated by LOCA accident (Loss of Cooling Accident) in combination with the subsequent events described in Pechova (2003). A large group of discharged radionuclides is taken into account (37 in total). The conclusion related to the performance of the multigroup scheme was verified.

8. Discussion and conclusions

A fast algorithm is presented for estimation of external irradiation from radioactive cloud nearby the source of pollution. The proposed unconventional finite cloud approach avoids the severe underestimation of cloudshine doses nearby the source arising from utilisation of the formerly used semi-infinite plume model. Thanks to its fast and effective operation this solution supports potency of the advanced consequence assessment techniques for improvement of emergency preparedness and management. The proposed method provides simulation of time and space evolution of cloudshine doses in the early phase of an accident in a real-time mode and on a detailed timescale. Large mixtures of discharged nuclides can be effectively treated simultaneously when the usual multi-nuclide approach is substituted by the new multi-group scheme. This software tool is incorporated into the routine operation of the environmental code HARP (HARP, 2011) with the aim for it to serve as a proper component supporting the advanced data assimilation techniques to be computationally feasible (Pecha et al., 2009; ASIM, 2012; Hofman et al., 2013). An experience with the particle filter sampling approximation was gained there for the solution of this complex task, which is analytically intractable.

Large uncertainties involved in an accident scenario and information noise occurring in the beginning of a calamity constitute a cardinal problem for the decision making staff. For example the uncertainty in the source term dominates among all other uncertainties of an accidental release scenario. Estimated radiological values can differ from the true ones by a factor of 10 or more. An improvement of the dose predictions in the specific nearest vicinity of the source of pollution taking into account the teledosimetric ring of sensors on fence of the nuclear power facility plays a decisive role in the source term re-estimation and inverse modelling. Such extraction of information from observations for the model parameter improvement increases credibility of the consequence assessment. The predictions of the potentially affected areas and the corresponding contamination levels can be recursively reconstructed.

Practically all advanced assimilation methods perform computationally expensive multiple repetitive recall of the environmental model. Hence the formulation of a fast and effective routine for determination of the external irradiation doses is of a crucial significance. It has to comply with other specific requirements in order to cover a large net of measuring apparatus located on the terrain which should include both fixed stations and various sensors on potential mobile vehicles. Furthermore, the routine is capable of managing the problem of a large mixture of discharging radionuclides when a new multi-group approach is introduced.

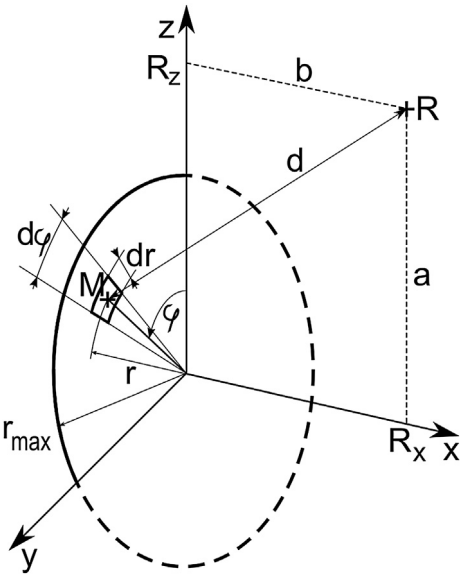

Fig. 8. Disc in plane (y, z) irradiating the receptor R.

This article addresses here only the cloudshine dose calculations. However, the measuring devices detect cloudshine and groundshine doses in total. For assimilation purposes a simplified assessment of contribution from the activity deposited on the ground (based on tabulated conversion factors) to the external irradiation has been applied (Pecha et al., 2009; Šmídl et al., 2013). In this conservative case an individual is assumed to be standing on a smooth infinite plane with a uniform source concentration. More detailed examinations should be related to additive modifying factors taking into account the effects of ground roughness and non-uniform source distribution. For these particular cases an effect of a possible near-standing shielding object should be taken into consideration.

Finally, it should be pointed out that the originated plume segmentation method based on the stepwise 2-D computational approach presented here can be considered a certain fast dispersion scheme alternative to the puff model.

Acknowledgements

These activities are supported thanks to Project No. VG20102013018, Ministry of the Interior of the Czech Republic.

Appendix A. Verification of the proposed algorithm for numerical integration

The photon fluence rate given by expression (3) is integrated numerically using the Gauss–Legendre integration formula which is the most commonly used form of Gaussian quadratures. The Gaussian quadratures provide the flexibility of choosing not only the weighting coefficients but also the locations (abscissas) where the function values are evaluated. The Gauss–Legendre formula is based on the Legendre polynomials of the first kind $P_m(x)$. For the chosen degree m of the polynomial we have tested the limits of its applicability on a given experimental configuration illustrated in Fig. 8.

An emitting disc with optional the radius r_{max} is located in the plane (y,z) with its centre in the origin of the coordinate system. We assume that without restriction to generality we can simplify the expression (3) in three manners:

- Uniform radioactivity concentration on the disc surface is assumed ($C(x, r, \varphi) = 1$ Bq/m^2)
- No photon absorption takes place in the medium between the disc and the receptor point R ($\mu = 0$)
- The photons are emitted from the disc elements isotropically and without any secondary collision on their path from the source up to the receptor point (the build-up factor is 1)

With exaggeration, it can be perceived as a "vacuum experiment" for the disc and receptors located in the outer space. Photon fluence rate (m^{-2} s^{-1}) is now expressed by simplified Equation (3):

$$\Phi(E_\gamma, R) = \frac{1}{4\pi} \int_{r=0}^{r_{max}} \int_{\varphi=0}^{2\pi} \frac{1}{d^2} r \mathrm{d}\varphi \mathrm{d}r \tag{14}$$

According to Fig. 8 the distance d between the sensor R and elemental surface $r \cdot \mathrm{d}\varphi \cdot \mathrm{d}r$ equals to

$$d = d(r, \varphi) = \sqrt{a^2 + b^2 + r^2 - 2 \cdot r \cdot a \cdot \cos\varphi}$$

Equation (14) can be integrated analytically and the number of photons crossing 1 m^2 per second at the position of the sensor R is expressed as:

$$\Phi(E_\gamma, R) = \frac{1}{4} \ln\left(\frac{r_{max}^2 + b^2 - a^2 + sqrt\left(r_{max}^4 + 2r_{max}^2 (b^2 - a^2) + (a^2 + b^2)^2 \right)}{2b^2} \right) \tag{15}$$

A 30-point Gauss–Legendre integration formula is used to numerically integrate Equation (14) for various ranges of constants a and b. A partial comparison of numerical and analytical values is presented in Table A1. Additional tests revealed a certain numerical instability for a case when the sensor R lies in the plane of the disc ($b = 0$) and constant a is approaching zero. In this instance we are using the lowest value of constant b slightly above zero ($b \cong 0.2$ m).

Table A1
Comparison of numerical and analytical values of photon fluence rate for various values a, b of sensor R positions. Radius of the radiating disc is $r_{max} = 49$ m.

a (m)	b (m)	Photon fluence rate Φ (m^{-2} s^{-1})	
		Analytically – see (15)	Numerically – see (14)
144	144	1.446555E-02	1.446555E-02
60	60	8.189546E-02	8.189548E-02
10	10	7.950500E-01	7.950501E-01
1.0	1.0	1.945767E+00	1.945910E+00
0.5	0.5	2.290156E+00	2.292484E+00
0.2	0.2	2.744151E+00	2.750629E+00
0.1	0.1	3.064821E+00	3.097203E+00

References

ADMS, 2009. Calculation of γ-Ray Dose Rate from Airborne and Deposited Activity. CERC Cambridge Environmental Research Cons. Ltd, Cambridge. ADMS4 P/20/01L/09.

Armand, P., Achim, P., Monfort, M., Carrere, J., Oldrini, O., Commanay, J., Albergel, A., 2005. Simulation of the plume gamma exposure rate with 3D Lagrangian particle model SPRAY and post-processor CLOUD-SHINE. In: Proc. 10th Int. Conf. On Harmonisation within Atm. Dispersion Modelling for Regulatory Purposes (Crete, Greece), pp. 545–550.

ASIM, 2012. ASIM – a Software Tool for Assimilation of Model Predictions with Observations from Terrain. URL: http://asim.utia.cas.cz/.

Bedwell, P., Wellings, J., Haywood, S.M., Hort, M.C., 2010. Cloud Gamma modelling in the UK MET Office's NAME III model. In: Proc 13th International Conference on Harmonisation within Atmospheric Dispersion Modelling for Regulatory Purposes (Paris, France), pp. 441–444.

Doucet, A., De Freitas, N., Gordon, N., 2001. Sequential Monte Carlo Methods in Practice. Springer Verlag.

HARP, 2011. HARP – Hazardous Radioactivity Propagation: a Software Tool for Fast Assessment of Radiological Consequences of Radiation Accident. URL: http://havarrp.utia.cas.cz/harp/.

Hanna, S., Briggs, R.G.A., Hosker Jr., R.P., 1982. Handbook on Atmospheric Diffusion. DOE/TIC-11223 (DE82002045).

Hofman, R., Pecha, P., 2011. Application of regional environmental code HARP in the field of off-site consequence assessment. In: PSA 2011 International Topical Meeting on Probabilistic Safety Assessment and Analysis. American Nuclear Society, Wilmington NC, USA.

ICRP, 1996. ICRP Publication 74 Ann. Conversion Coefficients for Use in Radiological Protection Against External Radiation, vol. 26. ICRP, pp. 3–4.

Overcamp, T.J., 2007. Solutions to the Gaussian cloud approximation for gamma absorbed dose. Health Phys. 92, 78–81.

Päsler-Sauer, J., 2000. Description of the Atmospheric Dispersion Model ATSTEP. RODOS(WG2)-TN(97)-01 KFK, Karlsruhe.

Pecha, P., Hofman, R., Šmídl, V., 2009. Bayesian tracking of the toxic plume spreading in the early stage of radiation accident. In: Proc. of European Simul. and Modelling Conference ESM.

Pecha, P., Pechova, E., 2002. Application of the COSYMA code for comparative analysis of a certain accidental releases of radioactivity. In: Proc. 4th International Conference IMUG2002 (Principality of Monaco), BNL Upton, pp. 5–15.

Pechova, E., 2012. Grouping of Gamma Rays According to Energies. Research report of Nuclear Research Institute Dpt. EGP Prague EGP 5014-F-120987.

Pechova, E., 2003. Calculation of Radioactivity Propagation – Joint Czech-Austrian Workshop, Vienna. Research report of Nuclear Research Institute Dpt. EGP Prague EGP 5014-J-030152.

RadDecay, 1996. Radioactive Nuclide Library and Decay Software – Version 1.13 for WINDOWS. Grove Engineering, Rockville, Maryland.

Raza, S.S., Avilla, R., Cervantes, J., 2001. A 3-D Lagrangian (Monte Carlo) method for direct plume gamma dose rate calculations. J. Nucl. Sci. Technol. 38 (4), 254–260.

Slade, D.M., 1968. Meteorology and Atomic Energy. USAEC TID 24190-1968, Russian translation.

Šmídl, V., Hofman, R., Pecha, P., 2013. Evaluation of detection abilities of monitoring networks using different assessment criteria. In: 15th Int. Conf. On Harmonisation within Atmospheric Dispersion Modelling for Regulatory Purposes (Madrid, Spain).

Smith, J.G., Simmonds, J.R. (Eds.), 2008. The Methodology for Assessing the Radiological Consequences of Routine Releases of Radionuclides to the Environment Used in PC-CREAM 08. Health Protection Agency, (Chilton, Didcot, UK). Research Report HPA-RPD-058.

Thykier-Nielsen, S., Deme, S., Láng, E., 1995. Calculation Method for Gamma Dose Rates from Gaussian Puffs. RISO National Laboratory, Roskilde, Denmark. RISO-R-775(EN).

Wang, X.Y., Ling, Y.S., Shi, Z.Q., 2004. A new finite cloud method for calculation external exposure dose in a nuclear emergency. Nucl. Eng. Des. 231, 211–216.